



Neuroendocrine Profile in a Rat Model of Psychosocial Stress: Relation to Oxidative Stress

Marilena Colaianna,^{1-3,*} Stefania Schiavone,^{2,3,*} Margherita Zotti,¹ Paolo Tucci,¹ Maria Grazia Morgese,¹ Liselotte Bäckdahl,⁴ Rikard Holmdahl,⁴ Karl-Heinz Krause,^{2,3} Vincenzo Cuomo,^{5,†} and Luigia Trabace^{1,†}

Abstract

Aims: Psychosocial stress alters the hypothalamic-pituitary-adrenal axis (HPA-axis). Increasing evidence shows a link between these alterations and oxidant elevation. Oxidative stress is implicated in the stress response and in the pathogenesis of neurologic and psychiatric diseases. NADPH oxidases (NOXs) are a major source of reactive oxygen species (ROS) in the central nervous system. Here, we investigated the contributory role of NOX2-derived ROS to the development of neuroendocrine alterations in a rat model of chronic psychosocial stress, the social isolation. **Results:** Significant elevations in the hypothalamic levels of corticotropin-releasing factor and plasmatic adrenocorticotrophic hormone were observed from 4 weeks of social isolation. Increased levels of peripheral markers of the HPA-axis (plasmatic and salivary corticosterone) were observed at a later time point of social isolation (7 weeks). Alteration in the exploratory activity of isolated rats followed the same time course. Increased expression of markers of oxidative stress (8-hydroxy-2-deoxyguanosine [8OhdG] and nitrotyrosine) and NOX2 mRNA was early detectable in the hypothalamus of isolated rats (after 2 weeks), but later (after 7 weeks) in the adrenal gland. A 3-week treatment with the antioxidant/NOX inhibitor apocynin stopped the progression of isolation-induced alterations of the HPA-axis. Rats with a loss-of-function mutation in the NOX2 subunit p47^{phox} were totally protected from the alterations of the neuroendocrine profile, behavior, and increased NOX2 mRNA expression induced by social isolation. **Innovation:** We demonstrate that psychosocial stress induces early elevation of NOX2-derived oxidative stress in the hypothalamus and consequent alterations of the HPA-axis, leading ultimately to an altered behavior. **Conclusion:** Pharmacological targeting of NOX2 might be of crucial importance for the treatment of psychosocial stress-induced psychosis. *Antioxid. Redox Signal.* 18, 1385–1399.

Introduction

PSYCHOSOCIAL STRESS IS KNOWN to determine the alterations of the physiological functioning of the hypothalamic-pituitary-adrenal axis (HPA-axis) (36) and to play a key role in the development of psychiatric diseases, such as psychosis (65). The HPA-axis represents the main neuroendocrine system for the regulation of the stress response (24). The paraventricular nucleus of the hypothalamus is the central element of this system, releasing mainly vasopressin and

corticotropin-releasing factor (CRF). These two hormones act on the pituitary gland, stimulating the secretion of adrenocorticotrophic hormone (ACTH), which, in turn, induces the production of glucocorticoid hormones (mainly cortisol in humans and corticosterone in rodents) from the adrenal gland. Alterations of the HPA-axis (mainly elevations in stress-related hormones) have been observed in psychotic patients (13, 21, 34) and in animal models of psychosis (8, 33). Increasing evidence has shown a role of oxidative stress in the control of the stress-response system, *via* several molecular

¹Department of Clinical and Experimental Medicine, University of Foggia, Foggia, Italy.

Departments of ²Pathology and Immunology and ³Genetic and Laboratory Medicine, Geneva University Hospitals, University of Geneva, Geneva, Switzerland.

⁴Department of Medical Biochemistry and Biophysics, Karolinska Institutet, Stockholm, Sweden.

⁵Department of Physiology and Pharmacology "Vittorio Erspamer," University of Rome "La Sapienza," Rome, Italy.

*These two authors have equally contributed to this work as co-first authors.

†These two authors have equally contributed to this work as co-last authors.

Innovation

Oxidative stress is involved in the neuroendocrine response to psychosocial stress and in the pathogenesis of psychiatric diseases. We demonstrate for the first time that psychosocial stress leads to early elevation of NADPH oxidase 2 (NOX2)-derived oxidative stress in the hypothalamus, determining alterations of the hypothalamic-pituitary-adrenal axis and leading ultimately to an altered behavior, reminiscent of psychotic symptoms in humans. Thus, pharmacological targeting of NOX2 might be of crucial importance for treatment of psychosocial stress-induced psychosis.

mechanisms, including altered translocation of the glucocorticoid receptors (9), elevation in the glutamate excitotoxicity (5), and alterations of RNA synthesis and stability (52). NADPH oxidase (NOX) enzymes are proteins that transfer electrons across the biological membranes to catalyze the reduction of molecular oxygen and generate the superoxide anion O_2^- (10). In the central nervous system (CNS), NOX isoforms are heterogeneously distributed in different regions and cell types, and thought to be involved in the regulation of cell fate and neuronal activity (55). From a pathologic point of view, NOX enzymes have been implicated in the generation of oxidative stress seen in a variety of brain disorders (55).

Animal models of mental disorders are essential tools to understand the molecular link between oxidative stress, alterations of the HPA-axis, and the development of psychiatric diseases. Recent evidence has shown that NOX2 is a major source of oxidative stress in the CNS, controlling alterations in neurotransmission and behavior (11, 53, 56) and the loss of phenotype of GABAergic interneurons (11, 53).

The social isolation rearing of rats is a model of chronic psychosocial stress that allows to study long-term alterations, reminiscent of symptoms of schizophrenic patients (23). A possible involvement of NOX2 in isolation-induced neuropathology and altered behavior has been recently shown (53).

A natural polymorphism of the *Ncf1* gene (referred in the text as a loss-of-function mutation), controlling the production of reactive oxygen species (ROS) by NOX2, is known in rats (46, 47). Importantly, a single-nucleotide polymorphism determines the functional effects. Indeed DA.*Ncf1*^{DA} rats with a lower capacity for ROS production (30, 46) differ only in the *Ncf1* gene from the congenic strain DA.*Ncf1*^{E3}. *Ncf1*, coding for the p47^{phox} protein, is an essential component of the NOX2/NOX complex, and a methionine instead of a threonine at position 153 reduces the capacity of oxidative burst by 40% (30). Importantly, the *Ncf1* polymorphism is widely occurring in wild rats and is therefore likely to result from natural selection (34).

Here, we investigate the role of NOX2-derived oxidative stress in the development of neuroendocrine alterations induced by psychosocial stress. We demonstrate a crucial early role of NOX2 in the disturbances of the HPA-axis, leading ultimately to psychotic diseases.

Results

Neuroendocrine and behavioral alterations induced by social isolation are time dependent

In control animals, hypothalamic levels of CRF, the plasmatic amount of ACTH, and the levels of salivary and plas-

matic corticosterone were stable over the 7-week period (Fig. 1A–D). In contrast, in isolated animals, a significant increase of the hypothalamic CRF and plasmatic ACTH levels was detected from 4 weeks of social isolation (Fig. 1A, B). While no changes in the levels of plasmatic and salivary corticosterone were found in control animals over the 7-week period, a significant increase of these markers was found in isolated animals at a later time point (after 7 weeks of social isolation) (Fig. 1C, D).

Pathological activation of the stress response in rodents is associated to an altered exploratory behavior (41, 59). While control animals were able to recognize the novel object from the familiar one over the 7-week period, the exploratory activity of isolated animals was compromised starting from 4 weeks of social isolation and worsened after 7 weeks (Fig. 1E).

Neuroendocrine and behavioral alterations induced by social isolation are associated to an early increase of oxidative stress in the hypothalamus

The presence of biomarkers of oxidative stress [e.g., 8-OHdG, one of the most abundant markers of DNA oxidation (14), and nitrotyrosine, an end product of NO-toxic species] was evaluated in the hypothalamus and in the adrenal glands. Thus, these two tissues have been associated with the central and peripheral control of the HPA-axis, respectively (45).

No change in the number of 8-OHdG- and nitrotyrosine-positive stained cells was detected in the hypothalamus and in the adrenal glands of control animals (Figs. 2A, G, 3A, E, and 4A, G, M, N). A significant early increase (after 2 weeks) of these two markers was detected in the hypothalamus of isolated animals (Figs. 2B, G and 3B, E), whereas the adrenal gland appeared to be affected only at later time points (from 7 weeks of social isolation) (Fig. 4B–F, H–L, M, N) both in the cortical and medullary regions (Fig. 4E, F, K, L). Confocal microscopy results for 8-OHdG and Neun, a neuronal-specific nuclear protein (44), 8OHdG and IBA-1, an ionized calcium-binding protein specifically expressed in microglia cells (2), 8OHdG and GFAP (glial fibrillary acidic protein) as a marker of astrocytes (22), nitrotyrosine and Neun, nitrotyrosine and IBA-1, and nitrotyrosine and GFAP show that in the hypothalamus of isolated rats, the large majority of 8OHdG-expressing cells were costained with *Neun* (Fig. 3F–H). In addition, the large majority of nitrotyrosine-expressing cells were costained with *Neun* (Fig. 2P–R). The large majority of both microglial cells and astrocytes were not involved in the increase of 8OHdG and nitrotyrosine (data not shown).

Social isolation induced no changes in the mRNA expression of *NOX1*, *NOX3*, and *NOX4*, both in the hypothalamus (Supplementary Fig. S1A–C; Supplementary Data are available online at www.liebertpub.com/ars) and in the adrenal glands (Supplementary Fig. S2A–C). Interestingly, *NOX2* mRNA expression showed the same time dependency observed for the biomarkers of oxidative stress, being significantly elevated at early time points in the hypothalamus (Fig. 3I) and at later time points in the adrenal glands (Fig. 4O).

The antioxidant/NOX inhibitor apocynin stops the progression of neuroendocrine alterations induced by social isolation

Apocynin prevents the behavioral and neuropathological alterations induced by 7 weeks of social isolation (53).

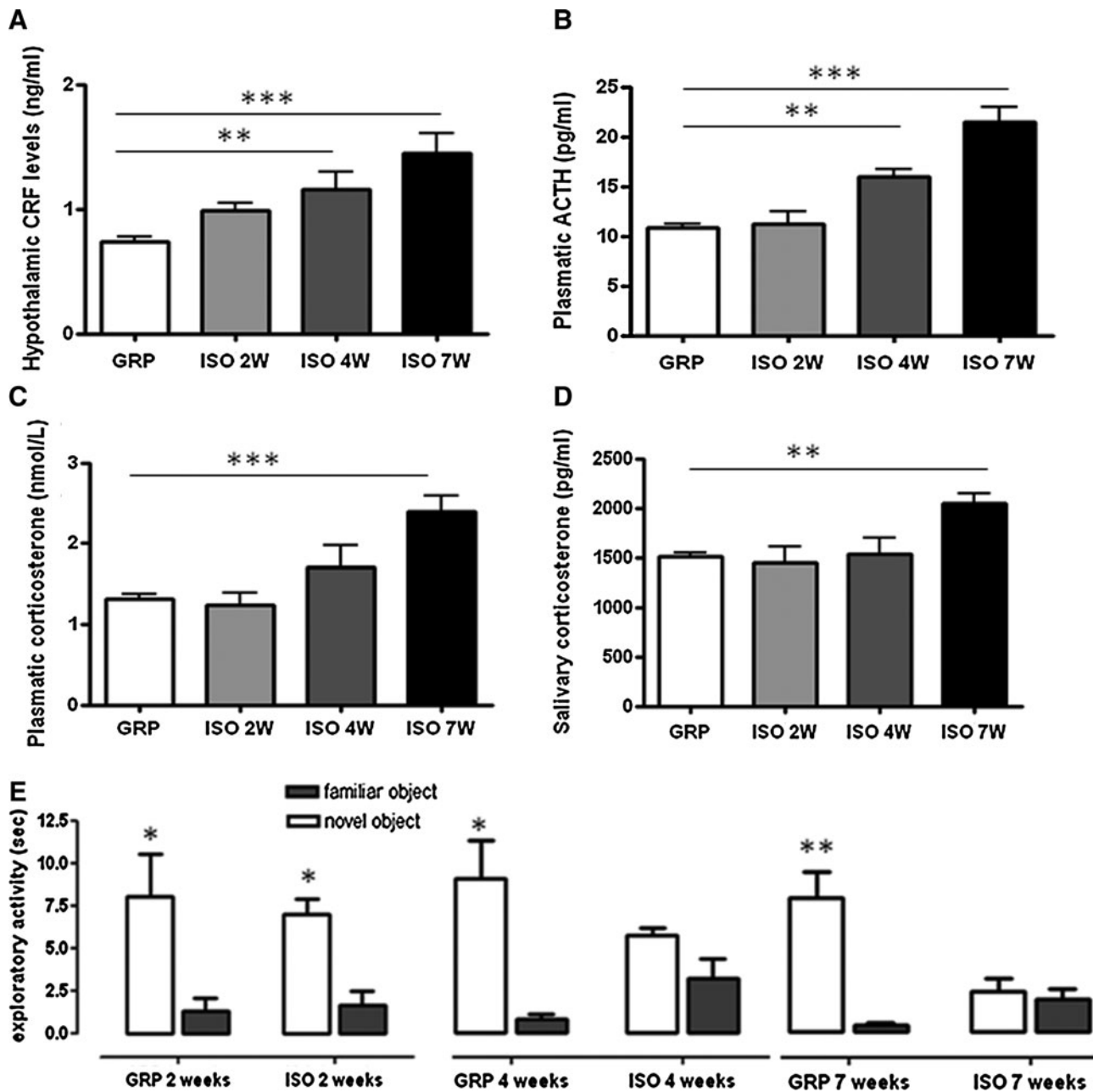


FIG. 1. Effects of social isolation on the HPA-axis functioning. **(A)** Hypothalamic levels of CRF (ng/ml) in GRP and ISO rats after 2 weeks (2W), 4 weeks (4W), and 7 weeks (7W) of social isolation ($n=5$ for each group in each time point). Statistical analysis: Two-way analysis of variance followed by Tukey *post hoc* test, r =rearing, t =time $F_{r(1,24)}=27.463$ $p<0.001$; $F_{t(2,24)}=2.480$ $p=0.105$; $F_{bxr(2,24)}=2.213$ $p=0.131$; $**p<0.01$; $***p<0.001$, not significant. $p=0.126$ ISO 2W versus GRP 2W; $p=0.969$, $p=0.998$, $p=0.982$ within GRP. **(B)** Plasmatic levels of ACTH (pg/ml) in GRP and ISO rats after 2W, 4W, and 7W of social isolation ($n=5$ for each group in each time point). Statistical analysis: Two-way analysis of variance followed by Tukey *post hoc* test, r =rearing, t =time $F_{r(1,24)}=40.128$ $p<0.001$; $F_{t(2,24)}=10.147$ $p<0.001$; $F_{bxr(2,24)}=13.890$ $p<0.001$; $**p<0.01$; $***p<0.001$, not significant $p=1$ ISO 2W versus GRP 2W; $p=0.852$, $p=0.961$, $p=0.961$ within GRP. **(C)** Plasmatic levels of corticosterone (nM) in GRP and ISO rats after 2W, 4W, and 7W of social isolation ($n=5$ for each group in each time point). Statistical analysis: Two-way analysis of variance followed by Tukey *post hoc* test, r =rearing, t =time $F_{r(1,24)}=11.962$ $p=0.002$; $F_{t(2,24)}=6.362$ $p=0.006$; $F_{bxr(2,24)}=6.543$ $p=0.005$; $***p<0.001$, not significant $p=0.797$ ISO 2W versus GRP 2W; $p=0.153$ ISO 4W versus GRP 4W, $p=0.963$, $p=0.963$, $p=1$; within GRP. **(D)** Salivary levels of corticosterone (pg/ml) in GRP and ISO rats after 2W, 4W, and 7W of social isolation ($n=5$ for each group in each time point). Statistical analysis: Two-way analysis of variance followed by Tukey *post hoc* test, r =rearing, t =time $F_{r(1,24)}=2.869$ $p=0.103$; $F_{t(2,24)}=3.574$ $p=0.044$; $F_{bxr(2,24)}=4.618$ $p=0.02$; $**p<0.01$, not significant $p=0.580$ ISO 2W versus GRP 2W; $p=0.951$ ISO 4W versus GRP 4W, $p=0.966$, $p=0.998$, $p=0.981$; within GRP. **(E)** Exploratory activity (sec) of the familiar and novel object in the Novel Object Recognition test of GRP and ISO rats after 2W, 4W, and 7W of social isolation ($n=8-10$ for each group in each time point). Statistical analysis: Student's *t*-test, $*p<0.05$ novel object versus familiar object within GRP 2W, ISO 2W, GRP 4W, and GRP 7W. not significant $p=0.896$ novel object versus familiar object within ISO 4W; $p=0.994$ novel object versus familiar object within ISO 7W. ACTH, adrenocorticotropic hormone; CRF, corticotropin-releasing factor; GRP, control rats (reared in group); HPA-axis, hypothalamic-pituitary-adrenal axis.

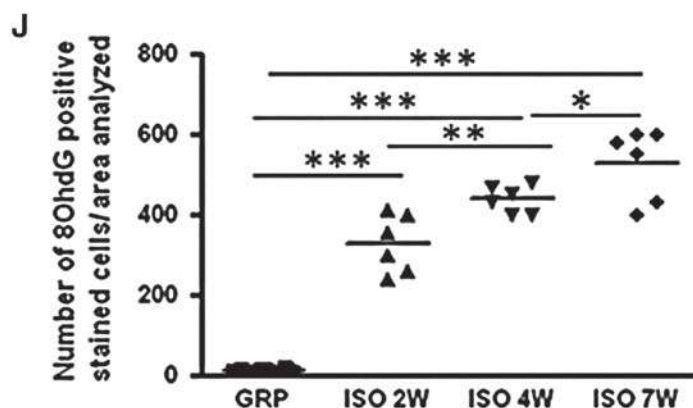
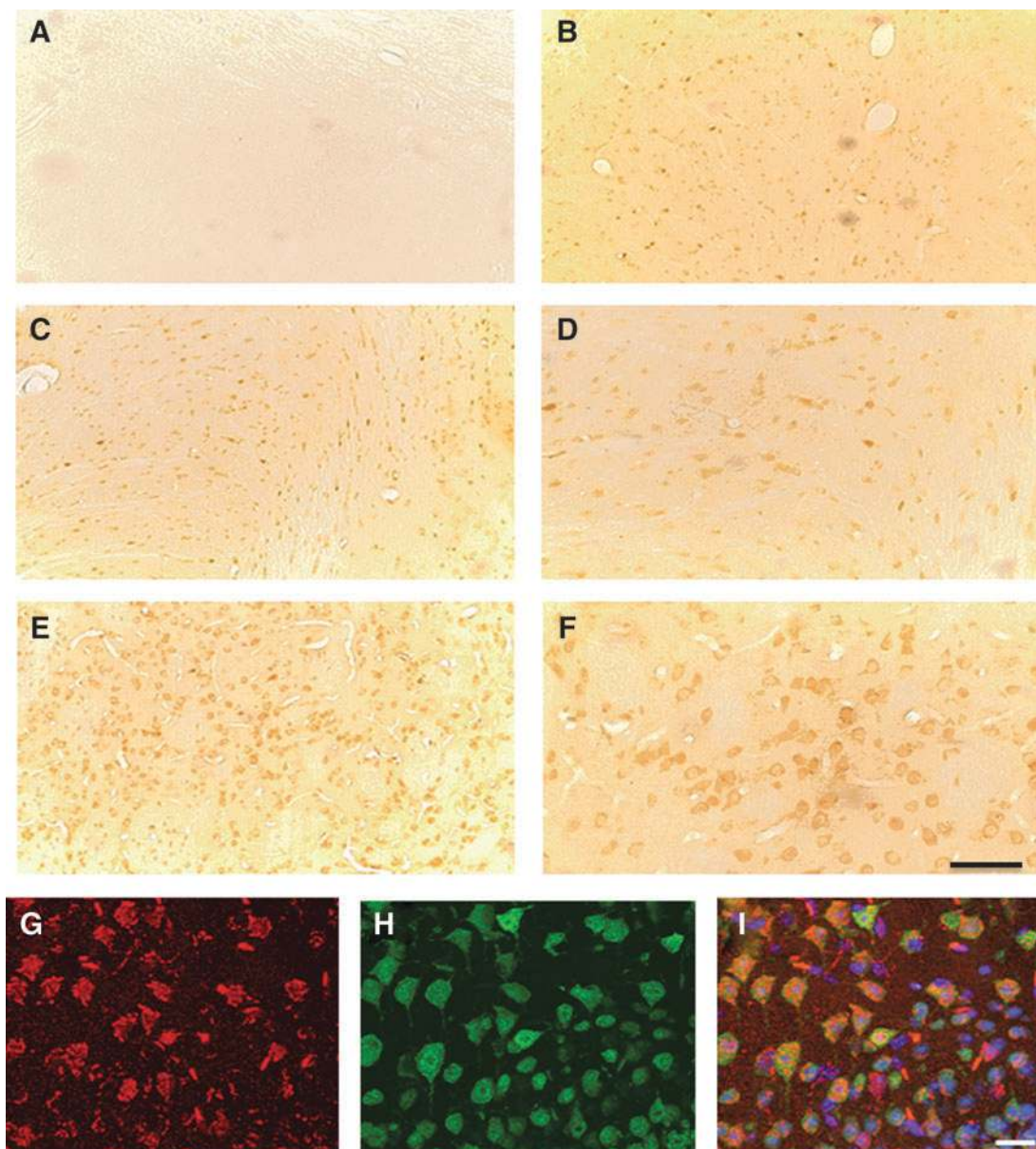


FIG. 2. Social isolation induces an early increase of oxidative stress (8OhdG) in the rat hypothalamus. (A–F) Representative images of DAB immunohistochemistry for 8OhdG in control (A) and isolated rats for a period of 2W (B), 4W (C, D), and 7W (E, F) of social isolation, ($n=6$ for each group in each time point). (D, F) are magnified views of (C, E), respectively. Scale bar: 55 μm . (G–I) Representative images of immunofluorescence (analyzed by confocal microscopy) for 8OhdG (red staining, G), NeuN (green staining, H), and merged with DAPI staining (I) in isolated animals ($n=6$ for each group in each time point). Scale bar: 54 μm . (J) Quantification of 8OhdG-immunoreactive cells in the hypothalamus of GRP and ISO rats after a period of 2W, 4W, and 7W ($n=6$ for each group in each time point). Statistical analysis: Two-way analysis of variance followed by Tukey *post hoc* test. $F_{(1,30)}=663.015$ $p<0.001$; $F_{(2,30)}=12.160$ $p<0.001$; $F_{\text{int}(2,30)}=12.864$ $*p<0.05$, $**p<0.01$, $***p<0.001$. 8OhdG, 8-hydroxy-2-deoxyguanosine.

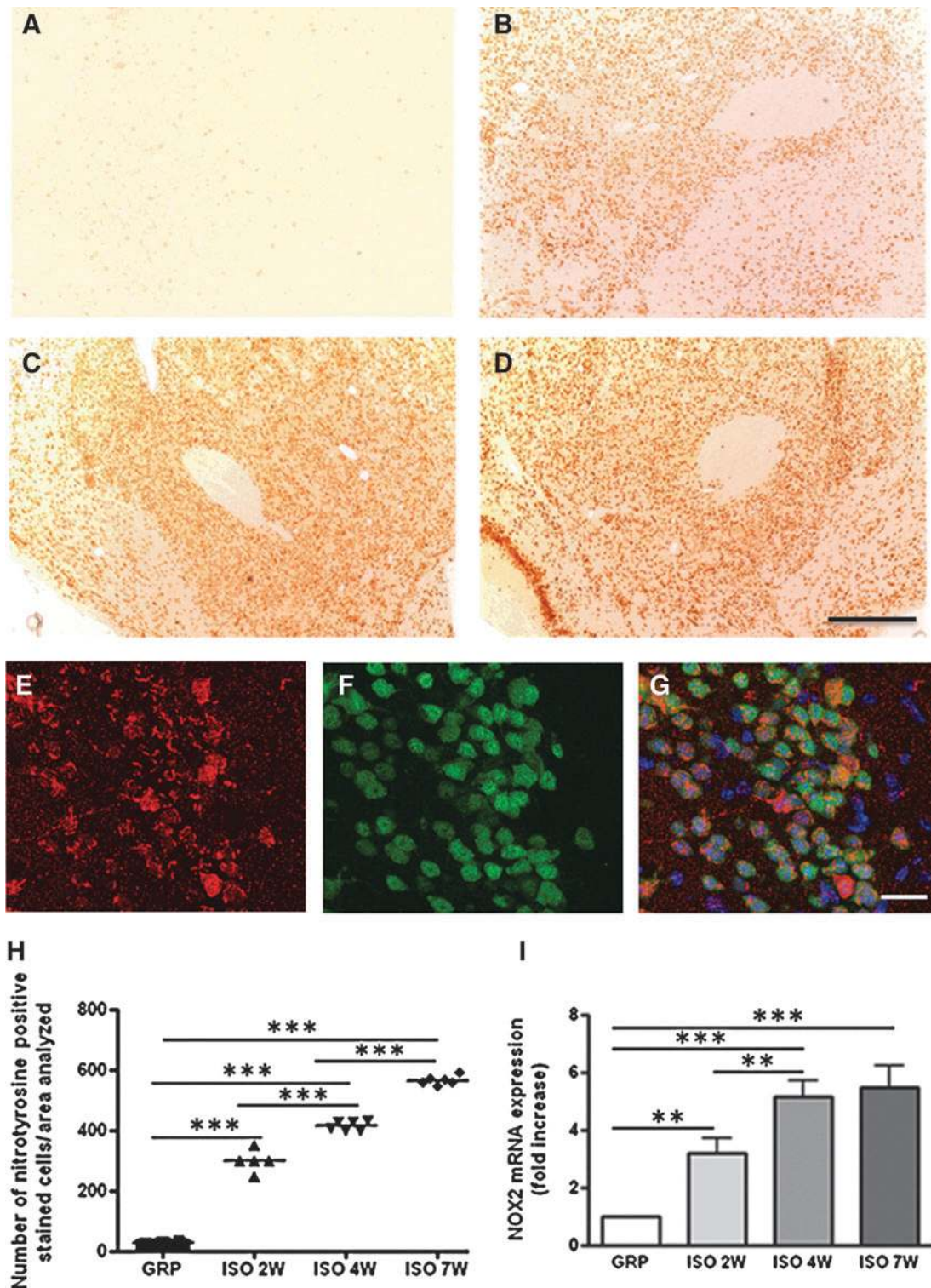


FIG. 3. Social isolation induces an early increase of oxidative stress (nitrotyrosine and NOX2) in the rat hypothalamus. (A–G) Representative images of DAB immunohistochemistry for nitrotyrosine in control (A) and isolated rats for a period of 2W (B), 4W (C), and 7W (D) of social isolation, ($n=6$ for each group in each time point). Scale bar: $50\ \mu\text{m}$. (E–G) Representative images of immunofluorescence (analyzed by confocal microscopy) for nitrotyrosine (red staining, E), NeuN (green staining, F), and a merged with DAPI (G) in isolated animals ($n=6$ for each group in each time point). (H) Quantification of nitrotyrosine immunoreactive cells in the hypothalamus of GRP and ISO rats after a period of 2W, 4W, and 7W ($n=6$ for each group in each time point). Statistical analysis: Two-way analysis of variance followed by Tukey *post hoc* test. $F_{r(1,30)}=586.675$ $p<0.001$; $F_{t(2,30)}=199.945$ $p<0.001$; $F_{\text{bxr}(2,30)}=211.987$ $p<0.001$; $***p<0.001$. (I) Real-time PCR for NOX2 mRNA expression (fold change) in the hypothalamus of GRP and ISO rats after a period of 2W, 4W, and 7W ($n=6$ for each group in each time point). Statistical analysis: Two-way analysis of variance followed by Tukey *post hoc* test. $F_{r(1,30)}=101,428$ $p<0.001$; $F_{t(2,30)}=4.116$ $p=0.026$; $F_{\text{bxr}(2,30)}=4.079$ $p=0.027$; $**p<0.01$; $***p<0.001$. NOX2, NADPH oxidase 2; PCR, polymerase chain reaction.

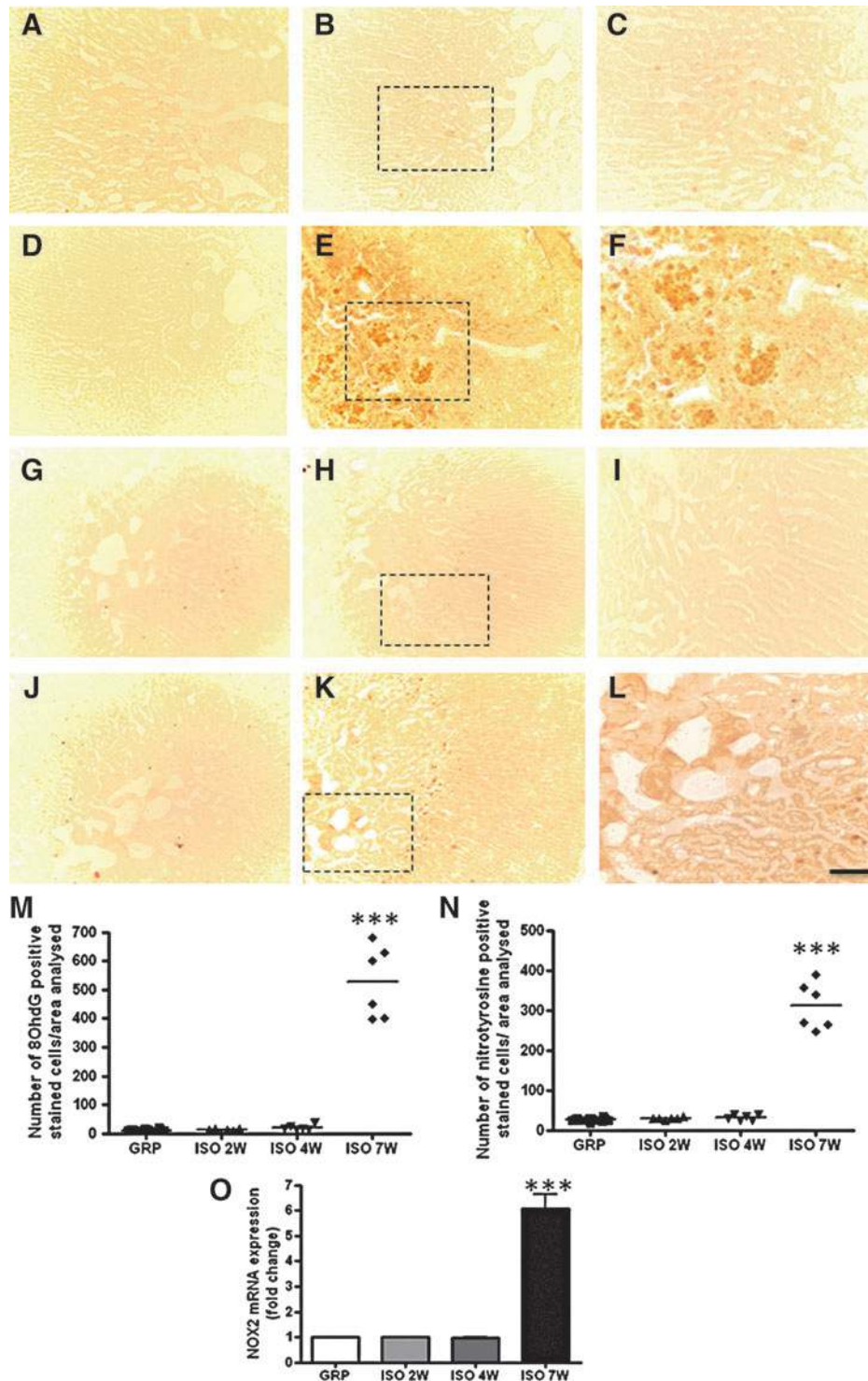


FIG. 4. Social isolation induces a late increase of oxidative stress in the rat adrenal gland. (A–F) Representative images of DAB immunohistochemistry for 8OhdG in control (A) and isolated rats for a period of 2W (B), 4W (D), and 7W (E) of social isolation, ($n=6$ for each group in each time point). (C, F) are magnified views of the *dotted box* in (B, E), respectively. (G–L) Representative images of DAB immunohistochemistry for nitrotyrosine in control (G) and isolated rats for a period of 2W (H), 4W (J), and 7W (K) of social isolation ($n=6$ for each group in each time point). (I, L) are magnified views of the *dotted box* in (H, K), respectively. (M) Quantification of 8OhdG-immunoreactive cells in the adrenal glands of GRP and ISO rats after a period of 2W, 4W, and 7W ($n=6$ for each group in each time point). Statistical analysis: Two-way analysis of variance followed by Tukey *post hoc* test. $F_{r(1,30)}=105.918$ $p<0.001$; $F_{t(2,30)}=98.500$ $p<0.001$; $F_{bcr(2,30)}=99.244$ $p<0.001$ $***p<0.001$, not significant; rearing within 2W $p=0.996$, rearing within 4W $p=0.701$. (N) Quantification of nitrotyrosine-immunoreactive cells in the adrenal glands of GRP and ISO rats after a period of 2W, 4W, and 7W ($n=6$ for each group in each time point). Statistical analysis: Two-way analysis of variance followed by Tukey *post hoc* test. $F_{r(1,30)}=149.028$ $p<0.001$; $F_{t(2,30)}=132.718$ $p<0.001$; $F_{bcr(2,30)}=137.412$ $p<0.001$; $***p<0.001$. (O) Real-time PCR for NOX2 mRNA expression (fold change) in the adrenal glands of GRP and ISO rats after a period of 2W, 4W, and 7W ($n=6$ for each group in each time point). Statistical analysis: Two-way analysis of variance followed by Tukey *post hoc* test. $F_{r(1,30)}=81.995$ $p<0.001$; $F_{t(2,30)}=81.996$ $p<0.001$; $F_{bcr(2,30)}=81.995$ $p<0.001$; $***p<0.001$. Scale bar: 58 μ M.

Hypothalamic CRF, plasmatic ACTH, and plasmatic and salivary corticosterone were analyzed in control and isolated animals at the end of weeks 4 and 7 (Fig. 5A). While apocynin had no effects on the HPA-axis of control animals, treatment with this compound was able to stop the progression of the neuroendocrine alterations. Indeed, (i) the biomarkers of the HPA-axis of isolated animals treated with apocynin were significantly decreased compared to the ones measured in the 7-week isolated animals not treated with apocynin (Fig. 5B–E); (ii) the biomarkers of the HPA-axis of isolated animals treated with apocynin did not differ from the ones measured in the set of animals isolated for 4 weeks not treated with apocynin (Fig. 5B–E).

Apocynin treatment was able to stop the progression of the increase of the hypothalamic 8OhdG levels and nitrotyrosine protein expression observed from week 4 to week 7 of the social isolation period (Fig. 5F, G). Three weeks of apocynin treatment also decreased the *NOX2* mRNA expression levels compared to the nontreated isolated rats (Fig. 5H).

Ncf1 polymorphism prevents neuroendocrine and behavioral alterations induced by social isolation

No basal differences in the hypothalamic CRF, plasmatic amount of ACTH, and plasmatic and salivary levels of corticosterone were observed between the Wistar strain and the DA strain (data not shown). Under control conditions, we did not detect any alteration in the markers of the HPA-axis between DA.*Ncf1*^{E3} and DA.*Ncf1*^{DA} rats (Fig. 6A–D). As described above for Wistar rats, 7 weeks of social isolation led to increased hypothalamic levels of CRF, plasmatic amount of ACTH, and plasmatic and salivary levels of corticosterone in the DA.*Ncf1*^{E3} strain. In contrast, social isolation had no impact on these biomarkers in DA.*Ncf1*^{DA} rats (Fig. 6A–D).

Ncf1 loss-of-function mutation also prevented the increase in the hypothalamic and adrenal 8OhdG levels (Fig. 6E–G) and nitrotyrosine protein expression (Fig. 6F) induced by 7 weeks of social isolation.

Exploratory activity of isolated DA.*Ncf1*^{E3} was strongly affected by 7 weeks of social isolation, while we did not detect the same negative impact of the social isolation on the exploratory activity of isolated DA.*Ncf1*^{DA} (Fig. 6H).

Seven weeks of social isolation induced a significant increase in the *NOX2* mRNA expression in the hypothalamus and adrenal glands of DA.*Ncf1*^{E3} rats, whereas this increase did not occur in DA.*Ncf1*^{DA} rats (Fig. 6I).

Increased HPA-axis functioning was observed in both DA.*Ncf1*^{E3}- and DA.*Ncf1*^{DA}-restrained rats (Supplementary Table. S1). Thus, the *Ncf1* polymorphism did not protect from the neuroendocrine alterations induced by acute stress.

Discussion

In this study, we investigated the time dependency of the HPA-axis alterations induced by psychosocial stress and its causal relationship with increased oxidative stress. We demonstrate that social isolation leads to an early elevation of *NOX2* expression and oxidative stress in the hypothalamus, followed by increase of CRF levels, plasmatic amount of ACTH, and an altered exploratory behavior. Elevations in the plasmatic and salivary levels of corticosterone, together with increased oxidative stress and *NOX2* mRNA expression in the adrenal gland, occur at later time points. A treatment with the

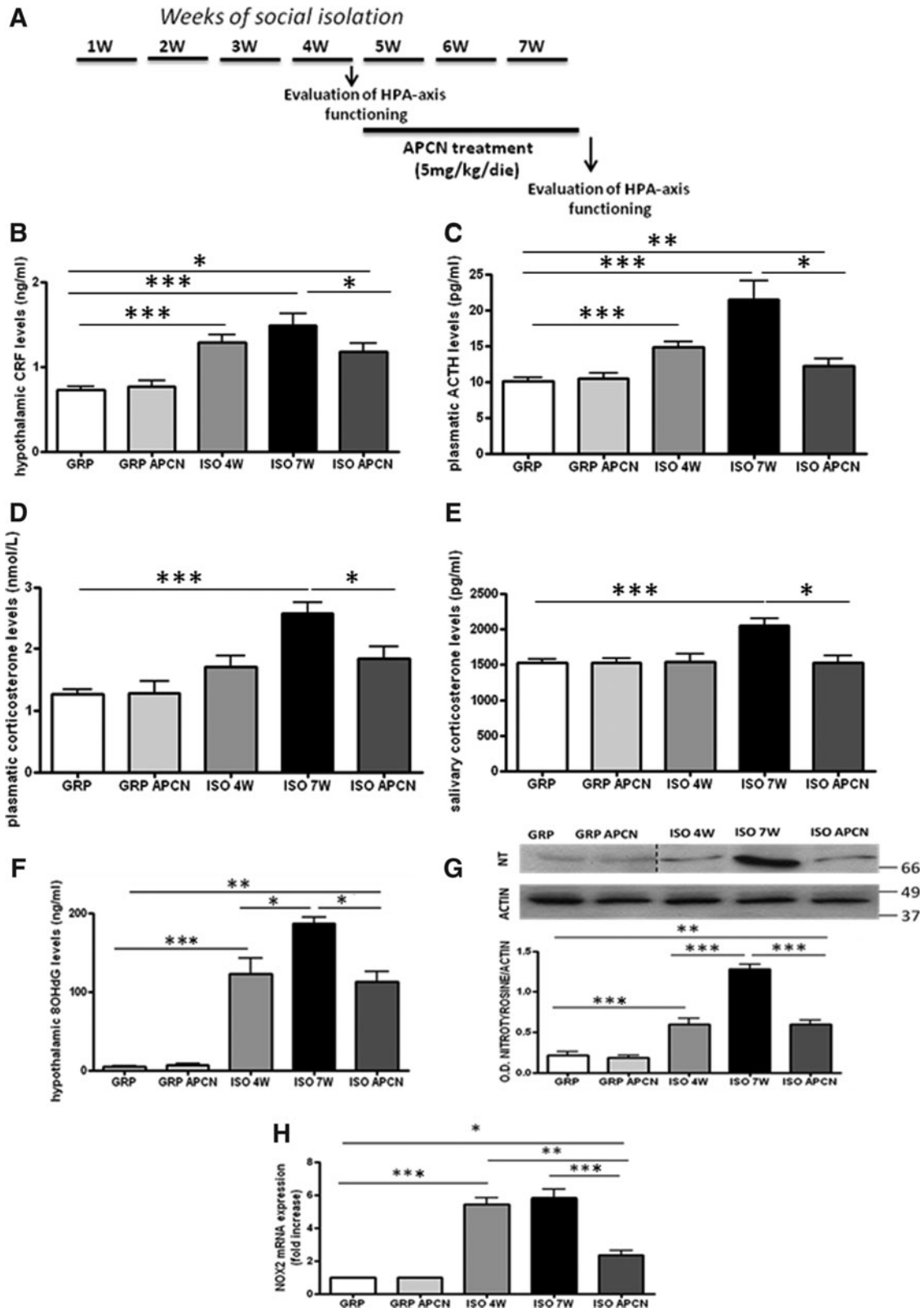
antioxidant/*NOX* inhibitor apocynin stops the progression of HPA-axis dysfunctions induced by social isolation, whereas a loss-of-function polymorphism in the *NOX2* subunit p47^{phox} completely prevents neuroendocrine and behavioral alterations, as well as the increase of *NOX2* expression in the hypothalamus and adrenal glands induced by social isolation.

To our knowledge, this is the first study showing a time course of the alterations of the HPA-axis and their relation to oxidative stress in the rat model of social isolation. Physiologically, both in humans and in rodents, the HPA-axis is not fully mature at birth. Indeed, there are several developmental changes occurring from childhood until late adolescence/early adulthood in both basal HPA activity and cortisol release (16, 26, 62). Referring specifically to the rat life, the three considered time points (2, 4, and 7 weeks after weaning) correspond to this critical period for the development of the neuroendocrine system going from childhood (2 weeks after weaning) toward adolescence (4 weeks after weaning) and early adulthood (7 weeks after weaning) (43, 54). Therefore, the responses observed at weeks 2 and 4 after weaning could be considered as an early response, because they involve the first stages of the development of the neuroendocrine system, while the responses observed at week 7 after the weaning could be considered as the late response, because it occurs in the last phase of this critical period of the HPA-axis development. We demonstrate that elevation in oxidative stress (*NOX2* mRNA expression and biomarkers of oxidative stress) is an early pathological event occurring in the hypothalamus, preceding the increase of CRF and plasmatic levels of ACTH. This finding is of crucial importance, given the central role of the hypothalamus in the stress response (50) and in the development of stress-related mental disorders (3). Thus, early neuropathological alterations of the hypothalamus have been shown in rodent models of chronic stress (7, 63) and in patients with mental disorders (19, 34). In this context, the early increase of oxidative stress and *NOX2* expression shown in our study might represent a triggering event of the stress response and HPA-axis activation.

Another novelty of the present work is the finding that the social isolation-induced increase of *NOX2* expression and oxidative stress in the adrenal gland (the peripheral component of the HPA-axis) is a late event. This might lead ultimately to an excessive release of corticosterone in the plasma (associated also with elevations in salivary corticosterone) and consequent worsening of an altered behavior. As well as the hypothalamus, the adrenal glands are also considered a key anatomical and physiological player in the response to psychosocial stress, given its crucial pathological role in rodent models of chronic stress (57, 64) and in patients with psychiatric disorders (17, 18, 38). However, to the best of our knowledge, no studies exist investigating specifically the temporal contribution of the increase of oxidative stress in the adrenal glands to the neuropathological response induced by chronic psychosocial stress. In this context, a possible, although still speculative, outline of the temporal events linking the increase of *NOX2*-derived oxidative stress to the HPA-axis dysfunctions might be as follows: chronic psychosocial stress might induce an early increase of *NOX2* expression and oxidative stress in the hypothalamus, leading first to increased release of the central biomarkers of the HPA-axis functioning (CRF and ACTH) and an altered exploratory behavior. The long-lasting elevation in *NOX2* expression and oxidative

stress in the hypothalamus, together with the appearance of elevations of *NOX2* expression and oxidative stress in the adrenal gland (at later time points), might determine the alterations in the peripheral biomarkers of the HPA-axis (plasma and salivary corticosterone) and, consequently,

worsening of the altered behavior. This outline is supported by recent evidence showing that increase in brain oxidative stress and/or reduced antioxidant defense has been found in the early phases of stress-induced mental disorders (39, 42, 48), and that both cerebral and peripheral long-lasting



oxidative stress is one of the main contributors to the worsening of the psychosocial stress-induced altered behavior in rodents (53, 56) and psychotic symptoms in humans (15, 35).

Mechanisms leading to NOX2 upregulation in neurons are not yet understood. In the ketamine mouse model of psychosis, neuronal production of interleukin-6 is necessary for the activation of NADPH oxidase in brain (12). Thus, it could be speculated that psychosocial stress leads to early activation of neuroinflammation in the hypothalamus, mediated by an increase of interleukin production and activation of microglial cells. Indeed, activated microglia after many different types of stimuli have been associated with NOX2 expression (28, 66). Release of mineralocorticoids, such as aldosterone, represents an important pathophysiological response to the activation of the HPA-axis, induced by psychosocial stress, and it is thought to be associated to increased oxidative stress in the adrenal glands (32, 49). Impairment in the aldosterone production rates has been found in depressive manic-depressive psychosis (29). Moreover, major depression has been found to occur in patients with elevated plasma concentrations of both cortisol and aldosterone after heart failure [reviewed in (25, 31)]. Treatment with spironolactone, an aldosterone antagonist, has been shown to attenuate this depression (1, 4). Thus, a role for aldosterone increase after elevation of oxidative stress induced by psychosocial stress could not be excluded from the above-described scenario.

In this study, we demonstrate the involvement of NOX2-derived oxidative stress in the development of neuroendocrine alterations and altered behavior by using a pharmacological approach. Although apocynin cannot be considered a specific NOX2 inhibitor rather than an antioxidant compound, its neuroprotective properties in neurodegenerative diseases (40, 60, 61, 67) and its role in the prevention of cell death after stroke have been recently shown (20). Apocynin effects have also been previously tested in rodent models of psychosis. Indeed, its prophylactic effect in the loss of phenotype of GABAergic neurons in the ketamine mouse model of psychosis (11, 12) and in the development of neuropathological and behavioral alterations in the rat model of social

isolation (53) has been reported. In the present study, we show a therapeutic effect of apocynin. Thus, administration of this compound (started when neuroendocrine alterations and altered behaviour begin to be detectable) stops the progression of the HPA-axis dysfunctions induced by social isolation. This finding might open innovative therapeutic insights for the treatment of the early phases of human psychosis. Treatment with apocynin also prevents the increase of NOX2 expression, induced by social isolation. This phenomenon could be explained by the fact that apocynin has not a direct effect on NOX2 enzyme transcription (6, 58). Thus, the block of NOX2 activation by apocynin might result in a decrease of NOX2 expression at mRNA levels, as a consequence of a homeostatic circuit.

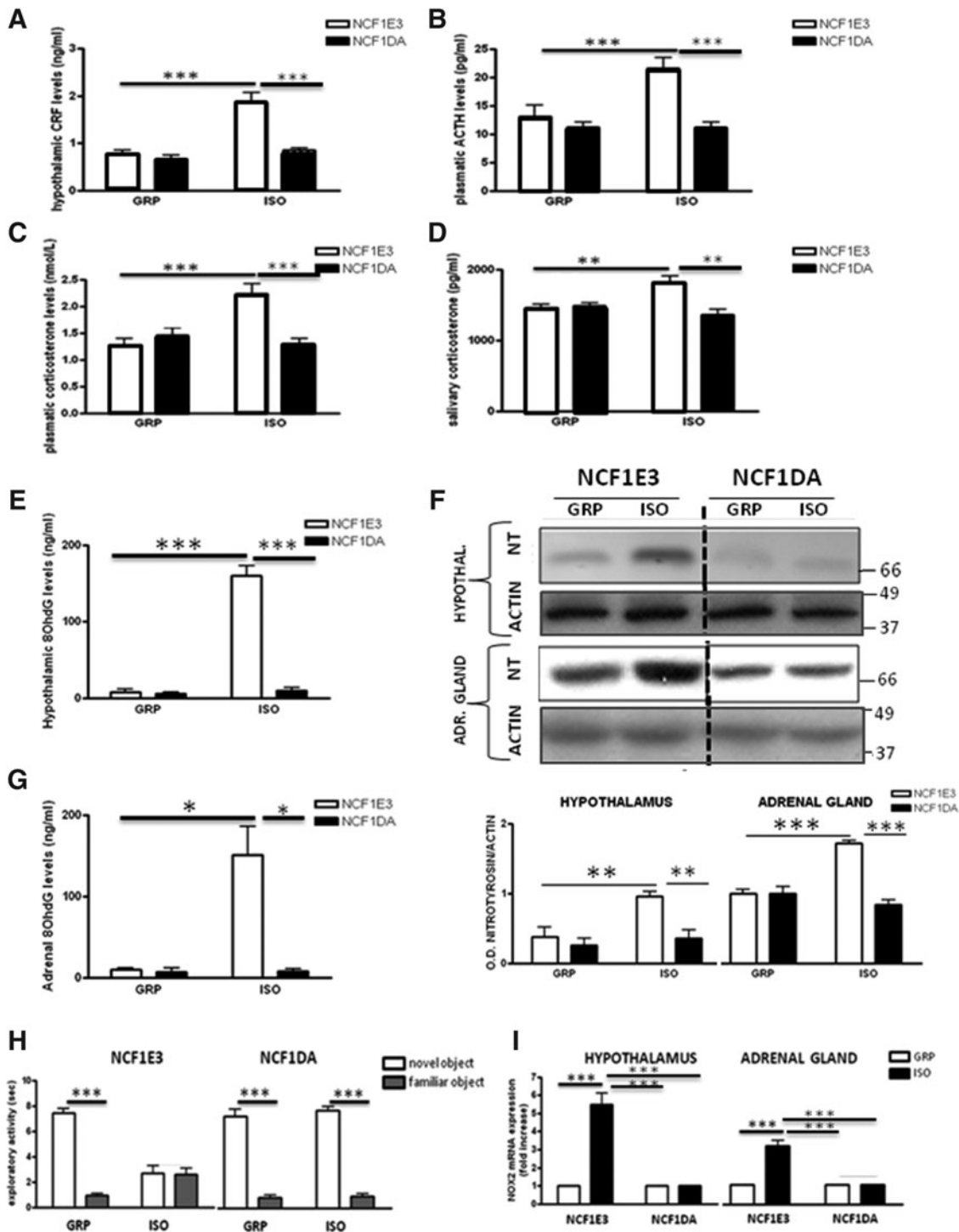
The data presented here provide an important genetic proof of principle of NOX2-derived oxidative stress involvement in the alterations of the HPA-axis and behavior induced by social isolation. Given the difficulties to obtain knockout rats, existence of rats with a loss-of-function mutation in the *Ncf1* gene, coding for the p47^{phox} subunit for NOX2, represents an important tool to verify the role of NOX2-derived oxidative stress in the development of neuroendocrine alterations induced by psychosocial stress. The exchange of a single amino acid (threonine to methionine at position 153) in the *Ncf1* allele leads to a lower oxidative burst (30, 46). The *Ncf1* locus is highly polymorphic in wild rats and the fully functional *E3* allele (with threonine at position 153) has dominant effects. More than half of the wild rat population (*Rattus norvegicus* trapped in Sweden and Germany) are homozygous for the *Ncf1*^{DA} alleles, having a low ROS response (46, 47). The data shown in Figure 5 of this article have been obtained by using inbred DA rats, polymorphic only with respect to the *Ncf1* locus. Thus, importantly, the total prevention of the development of neuroendocrine alterations induced by chronic social stress is due to a single-nucleotide polymorphism. Interestingly, the *Ncf1* polymorphism does not confer protection from the increased release of the central and peripheral biomarkers of the HPA-axis functioning induced by acute stress. Indeed, the neuroendocrine response of

FIG. 5. Effects of 3W of apocynin (APCN) treatment on the alterations of the HPA-axis functioning induced by social isolation. (A) Schematic representation of the treatment protocol with APCN treatment (5 mg/kg/die) during the last 3W of social isolation. **(B–E)** Effects of 3-week APCN treatment on the levels of the four markers of HPA-axis functioning in GRP and ISO rats. $n = 10$ for GRP 4W; 5 for GRP 7W; 5 for GRP 4W + 3W APCN; 10 for ISO 4W; 5 for ISO 7W; 5 for ISO 4W + 3W APCN. Three-way ANOVA followed by Tukey *post hoc* test; r=rearing, t=time, tr=treatment. For CRF, $F_{r(1,40)} = 118.71$ $p < 0.001$; $F_{tr(1,40)} = 1.863$ $p = 0.180$; $F_{t(1,40)} = 0.295$ $p = 0.590$; $F_{rxtr(1,40)} = 3.470$ $p = 0.070$; $F_{rxt(1,40)} = 1.084$ $p = 0.304$; $F_{trxt(1,40)} = 1.134$ $p = 0.293$; $F_{rxtrxt(1,40)} = 4.679$ $p = 0.037$; * $p < 0.05$; *** $p < 0.001$. For plasmatic ACTH, $F_{r(1,40)} = 70.105$ $p < 0.001$; $F_{tr(1,40)} = 11.246$ $p < 0.01$; $F_{t(1,40)} = 2.491$ $p = 0.122$; $F_{rxtr(1,40)} = 11.246$ $p < 0.01$; $F_{rxt(1,40)} = 0.233$ $p = 0.632$; $F_{trxt(1,40)} = 11.246$ $p < 0.01$; $F_{rxtrxt(1,40)} = 11.246$ $p < 0.01$; * $p < 0.05$; ** $p < 0.01$; *** $p < 0.001$. For plasmatic corticosterone, $F_{r(1,40)} = 124.987$ $p < 0.001$; $F_{tr(1,40)} = 4.414$ $p < 0.05$; $F_{t(1,40)} = 0.002$ $p = 0.963$; $F_{rxtr(1,40)} = 4.414$ $p < 0.05$; $F_{rxt(1,40)} = 3.046$ $p = 0.089$; $F_{trxt(1,40)} = 4.414$ $p < 0.05$; $F_{rxtrxt(1,40)} = 4.414$ $p < 0.05$; * $p < 0.05$; *** $p < 0.001$. For salivary corticosterone, $F_{r(1,40)} = 17.823$ $p < 0.001$; $F_{tr(1,40)} = 5.284$ $p < 0.05$; $F_{t(1,40)} = 0.0676$ $p = 0.796$; $F_{rxtr(1,40)} = 5.284$ $p < 0.05$; $F_{rxt(1,40)} = 3.047$ $p = 0.089$; $F_{trxt(1,40)} = 5.284$ $p < 0.05$; $F_{rxtrxt(1,40)} = 5.284$ $p < 0.05$; * $p < 0.05$; *** $p < 0.001$. **(F)** Hypothalamic 8OhdG levels (ng/ml) assessed by ELISA in GRP and ISO animals treated according to the protocol shown in Figure 4A. $F_{r(1,40)} = 289.252$ $p < 0.001$; $F_{tr(1,40)} = 6.083$ $p < 0.05$; $F_{t(1,40)} = 3.922$ $p = 0.054$; $F_{rxtr(1,40)} = 5.473$ $p < 0.05$; $F_{rxt(1,40)} = 2.406$ $p = 0.128$; $F_{trxt(1,40)} = 5.551$ $p < 0.05$; $F_{rxtrxt(1,40)} = 6.001$ $p < 0.05$; * $p < 0.05$; ** $p < 0.01$; *** $p < 0.001$. **(G)** Representative images of western blotting for nitrotyrosine and actin in the hypothalamus of GRP and ISO rats treated according to the protocol shown in Figure 4A with optical density (OD) protein bands normalized to the actin protein values. $F_{r(1,40)} = 236.385$ $p < 0.001$; $F_{tr(1,40)} = 21.171$ $p < 0.001$; $F_{t(1,40)} = 17.242$ $p < 0.001$; $F_{rxtr(1,40)} = 21.171$ $p < 0.001$; $F_{rxt(1,40)} = 25.504$ $p < 0.001$; $F_{trxt(1,40)} = 21.171$ $p < 0.001$; $F_{rxtrxt(1,40)} = 21.171$ $p < 0.001$; ** $p < 0.01$; *** $p < 0.001$. **(H)** Real-time PCR for NOX2 mRNA expression (fold change) in the hypothalamus of GRP and ISO rats treated according to the protocol shown in Figure 4A. $F_{r(1,40)} = 305.401$ $p < 0.001$; $F_{tr(1,40)} = 15.951$ $p < 0.001$; $F_{t(1,40)} = 10.586$ $p < 0.01$; $F_{rxtr(1,40)} = 15.951$ $p < 0.001$; $F_{rxt(1,40)} = 10.586$ $p < 0.01$; $F_{trxt(1,40)} = 15.951$ $p < 0.001$; $F_{rxtrxt(1,40)} = 15.951$ $p < 0.001$; * $p < 0.05$; ** $p < 0.01$; *** $p < 0.001$.

rats with low oxidative burst to 60 min of restraint stress does not differ from the response of rats with high oxidative burst to the same acute stress. How these results could be explained in the context of stress response in wild nature? It is possible that exposure to acute stress in nature leads to an immediate increase of oxidative stress and activation of the HPA-axis to assure the fight-or-fly response (51). On the other hand, the effects of the *Ncf1* polymorphism might represent a form of adaptation to long-lasting stress, needing more time to be evident and, therefore, not detectable in the immediate

response to an acute stress. Thus, the *Ncf1* polymorphism might be a crucial new candidate in the understanding of the mechanisms leading to the positive adaptation and to the ability to maintain or regain mental health (despite experiencing severe adversity), also known as resilience (27).

In conclusion, we provide evidence for a key role of early NOX2-derived oxidative stress in the development of neuroendocrine alterations induced by psychosocial stress. Our results suggest that NOX2 might represent a crucial molecular link between HPA-axis dysfunctions and mental disorders.



Therefore, targeting NOX2 enzyme might provide innovative approaches for the cure of psychiatric diseases.

Materials and Methods

Animals

An equal number of adult male and female Wistar rats (Harlan, S. Pietro al Natisone), DA (with the ROS-low responder *Ncf1^{DA}* allele) and DA.Pia4 (with the ROS high-responder *Ncf1^{E3}* allele) (Medical Inflammation Research animal house, Karolinska Institute, Stockholm) rats were used to obtain litters. All animals were housed at a constant room temperature (22°C ± 3°C) and a relative humidity (55% ± 5%) under a 12-h light/dark cycle (lights on from 7:00 AM to 7:00 PM). Food and water were freely available. All efforts were made to minimize the number of animals used and their suffering in conformity with the ethics guidelines and national and international laws (DL Number 116, G. U, suppl. 40, 18 February 1992, Circolare Number 8, GU, July 14, 1994; EEC Council Directive 86/609, OJ L 358, December 1, 2012, 1987; Guide for the Care and Use of Laboratory Animals, U.S. National Research Council, 1996).

Genotyping of animals

The 3 DA/E3 single nucleotide polymorphisms (snps) in *Ncf1* were genotyped by the high-resolution melt curve analysis. First, DNA was purified from tail tips using a DNeasy DNA isolation kit from Qiagen. The primers for the HRM single nucleotide polymorphism (snp) typing were designed using primer express software, and the sequences were as follows:

Ncf1exon4_R GGTGGCTACTCACTGGCTGT;
Ncf1exon4_F CCGAGTACTTCAACAGCCTCA;
Ncf1exon 6_F TGGCCCGATAGGTCTGAAG;
Ncf1exon 6_R CCCTGCTGTGCCATTCA;
Ncf1exon 11_F ACACGGCGGACGTCAGTT;
Ncf1exon 11_R ACCCAGCTCGGACCTCATC.

HRM curve analysis was performed in a BIORAD C1000 thermal cycler immediately after a 40-cycle amplification using Sso-fast evagreen cybermix from Biorad and the annealing temperature 60 degrees. To determine the allelic melting con-

dition for differentiation between the DA and E3 alleles of the three snps, the real-time polymerase chain reaction (PCR) products were subjected to the ramping of 0.1°C/s between 83°C and 94°C. All specimens were tested in triplicate, and their melting profiles analyzed using Biorad HRM melt software. Control homozygous DA, homozygous E3, and the DA/E3 heterozygous were used as standards for the melting-temperature curve classification. For the standards, each allelic-variant melt curve was set as a genotype, and the samples were classified as either DA or E3 according to their melt curve.

All Wistar rats used in this study were genotyped, and all of them had the *Ncf1^{E3}* allele, thus with a higher ROS response (data not shown).

Social isolation protocol

The social isolation procedure (37) was performed on male rats. At weaning (postnatal day 21), pups were separated from their mothers and reared either as isolated rats (ISO; one rat per cage) or in social groups [control rats (reared in group), GRP; three to four rats per cage]. To avoid a litter effect, each litter contributed only one subject to the GRP and one subject to the ISO. All animals were reared in Plexiglas cages (ISO: 48.0 × 27.0 × 20.0 cm; GRP: 59.0 × 38.5 × 20.0 cm). Animals exposed to 2 weeks of social isolation were 5 weeks old; animals exposed to 4 weeks of social isolation were 7 weeks old; and animals exposed to 7 weeks of social isolation were 10 weeks old. Animals were disturbed only for cleaning purposes, which consisted of changing the cage once a week for ISO and twice a week for GRP. Both ISO and GRP rats were housed in the same room, so that ISO rats maintained a visual, auditory, and olfactory contact with the other animals.

Blindness of the study. Researchers performing behavioral, histological, and biochemical analysis were blind with respect to the rearing and treatment conditions. Indeed, it was not possible to deduce from the labeling whether an animal was isolated or not. The social isolation procedure was performed in a dedicated part of the animal facility, not accessible to the investigators during the entire period of the social isolation protocol. The blinding of the data was maintained until the analysis was terminated.

FIG. 6. The *Ncf1* mutation protects from the neuroendocrine alterations induced by social isolation. (A) Hypothalamic levels of CRF (ng/ml) in *Ncf1^{E3}* and *Ncf1^{DA}* GRP and ISO for 7W ($n=6$ for each group in each time point). Two-way ANOVA followed by Tukey *post hoc* test. r =rearing, g =genotype $F_{r(1,20)}=26.355$ $p<0.001$; $F_{g(1,20)}=19.878$ $p<0.001$; $F_{txg(1,20)}=12.526$ $p=0.002$; $***p<0.001$. **(B)** Plasmatic levels of ACTH (pg/ml) in *Ncf1^{E3}* and *Ncf1^{DA}* GRP and ISO for 7W ($n=6$ for each group in each time point). $F_{r(1,20)}=26.355$ $p<0.001$; $F_{g(1,20)}=19.878$ $p<0.001$; $F_{txg(1,20)}=12.526$ $p=0.002$; $***p<0.001$. **(C)** Plasmatic levels of corticosterone (nM) in *Ncf1^{E3}* and *Ncf1^{DA}* GRP and ISO for 7W. $F_{r(1,20)}=7.101$ $p=0.015$; $F_{g(1,20)}=7.101$ $p=0.015$; $F_{txg(1,20)}=15.517$ $p<0.001$; $***p<0.001$. **(D)** Salivary levels of corticosterone (pg/ml) in *Ncf1^{E3}* and *Ncf1^{DA}* GRP and ISO for 7W. $F_{r(1,20)}=2.139$ $p=0.159$; $F_{g(1,20)}=7.911$ $p=0.011$; $F_{gxr(1,20)}=10.646$ $p=0.004$; $**p<0.01$. **(E)** Hypothalamic 8OHdG levels (ng/ml) assessed by ELISA in *Ncf1^{E3}* and *Ncf1^{DA}* GRP and ISO for 7W. $F_{r(1,20)}=126.664$ $p<0.001$; $F_{g(1,20)}=120.259$ $p<0.001$; $F_{gxr(1,20)}=114.072$ $p<0.001$; $***p<0.001$. **(F)** Representative images of western blotting for nitrotyrosine and actin in the hypothalamus and the adrenal glands of *Ncf1^{E3}* and *Ncf1^{DA}* GRP and ISO for 7W with optical density (OD) protein bands normalized to the actin protein values. $F_{r(1,20)}=16.960$ $p<0.001$; $F_{g(1,20)}=15.486$ $p<0.001$; $F_{gxr(1,20)}=7.044$ $p<0.05$; $**p<0.01$. For adrenal gland, $F_{r(1,20)}=24.020$ $p<0.001$; $F_{g(1,20)}=47.078$ $p<0.001$; $F_{gxr(1,20)}=59.314$ $p<0.001$; $***p<0.001$. **(G)** Adrenal 8OHdG levels (ng/ml) assessed by ELISA in *Ncf1^{E3}* and *Ncf1^{DA}* GRP and ISO for 7W. $F_{r(1,20)}=26.355$ $p<0.001$; $F_{g(1,20)}=19.878$ $p<0.001$; $F_{gxr(1,20)}=12.526$ $p<0.01$; $*p<0.05$. **(H)** Exploratory activity (sec) of the familiar and novel object in *Ncf1^{E3}* and *Ncf1^{DA}* GRP and ISO for 7W. Student's *t*-test, $***p<0.001$ novel object *versus* familiar object within *Ncf1^{E3}* GRP, *Ncf1^{DA}* GRP, and *Ncf1^{DA}* ISO. **(I)** Real-time PCR for NOX2 mRNA expression (fold change) in the hypothalamus and the adrenal glands of *Ncf1^{E3}* and *Ncf1^{DA}* c GRP and ISO for 7W. $F_{r(1,20)}=51.718$ $p<0.001$; $F_{g(1,20)}=50.964$ $p<0.001$; $F_{gxr(1,20)}=50.216$ $p<0.001$; $**p<0.01$. For adrenal gland, $F_{r(1,20)}=45.882$ $p<0.001$; $F_{g(1,20)}=45.885$ $p<0.001$; $F_{gxr(1,20)}=45.789$ $p<0.001$; $***p<0.001$.

Apocynin treatment

Apocynin treatment (5 mg/kg/day in drinking water) was applied to the control and isolated animals, as previously described (7, 40), from week 4 to week 7 of social isolation.

Acute restraint stress

Rats were transported to the experimental room in their home cages and allowed to adapt to this environment for at least 30 min. Animals were then submitted to a 60-min restraint period in a plastic cylindrical restraining tube (diameter 6.5 cm and length 15 cm). After restraint, the animals returned to their cages.

Measurement and quantification of markers of the HPA-axis

CRF. Rats were killed by decapitation, and the brain was immediately removed for hypothalamus dissection. Tissues were frozen and stored at -80°C until the analysis was performed. Hypothalamic CRF concentrations (ng/ml) were determined using a commercial ELISA kit (CRF Rat/Mouse Sensitive ELISA Kit; Biovendor).

Plasmatic ACTH and corticosterone. Blood was collected from the trunk of killed rats into heparinized tubes and then centrifuged at $10,000 g$ for 20 min at 4°C . The supernatants were removed and frozen at -80°C until the analysis was performed. Plasmatic ACTH concentrations (pg/ml) were determined using a commercial ELISA kit (ACTH Rat/Mouse Ultrasensitive lumELISA; Demeditec Diagnostics). Plasmatic corticosterone levels (nM) were determined using a commercial ELISA kit (Corticosterone ELISA kit; Abnova, DBA Italia S.r.l. and Corticosterone EIA kit; Alexis Biochemical, Vinci-Biochem).

Salivary corticosterone. Salivary samples were collected in plastic tubes after intraperitoneal injection of pilocarpin (5 mg/kg). The absence of blood contamination was checked using a salivary blood contamination kit (Salimetrics Europe Ltd.). Samples were stored at -80°C until they were assayed after a proper dilution (1:16) with an assay buffer.

The salivary corticosterone (pg/ml) levels were determined using a commercial ELISA kit (Corticosterone ELISA kit; Abnova, DBA Italia S.r.l. and Corticosterone EIA kit; Alexis Biochemical, Vinci-Biochem).

Measurement and quantification of markers of oxidative stress

Hypothalamic and adrenal 8OHdG (ng/ml) were determined using a commercial ELISA kit (Highly Sensitive 8-OHdG Check Elisa; JaiCa). The hypothalamic and adrenal nitrotyrosine protein expression levels were determined by Western blotting, as previously described (Schiavone *et al.*), using a rabbit polyclonal anti-nitrotyrosine antibody (1:100; Millipore) and α -actin (1:4000; Sigma-Aldrich). The antibody we used to detect nitrotyrosine protein revealed one major band at ~ 67 kDa. Other very weak bands are present in the background of the blot. The optical density measurements refer only to the major band of the blot.

Optical densities of the bands were measured using ImageJ software (<http://rsb.info.nih.gov/ij/>) and normalized with α -actin.

Novel-object recognition test

Rats were exposed to two habituation sessions (intersession interval: 24 h) where they were allowed 5 min to explore the apparatus. Twenty-four h after the last habituation, two 3-min trials separated by a 1-min intertrial interval were carried out. In the first trial, rats were exposed to two identical objects (white glasses or light bulbs). During the second trial, rats were exposed to one familiar object and to a new, differently shaped object. Each object was placed at an equidistant position between the center and the wall of the arena. At the beginning of each trial, the rats were placed in the center of the arena with their heads oriented in the opposite direction to the objects. Exploration of the objects was defined as sniffing or touching the object with the nose. Turning around or sitting on the object was not considered as exploration. Exploratory activity was expressed as time (sec) of exploration. Objects and arena were carefully cleaned between each session to avoid confounding olfactory stimuli.

Immunohistochemistry

Immunohistochemical analyses were performed in the hypothalamus and in the adrenal glands as previously described (53, 56), using monoclonal and polyclonal antibodies against 8OHdG (1:10; JaiCa), nitrotyrosine (1:100; Millipore), Neun (1:2000; Chemicon), Iba-1 (1:500; Wako), and GFAP (1:2000; Millipore).

Quantifications of immunohistochemistry have been performed using Metamorph software (Molecular Devices) and expressed as the number of positive-stained cells per area analyzed. Concerning the 8OHdG and nitrotyrosine immunostaining experiments in the hypothalamus, the mean of the total number of cells per field was around 800. No differences were detected in the total number of cells per field among experimental groups (Supplementary Fig. S3A, B). The magnification used for the quantification was $20\times$, and the number of fields studied for the sample was four. No differences were found in the total cell numbers among analyzed fields per sample (data not shown). Concerning 8OHdG and nitrotyrosine immunostaining experiments in the adrenal glands, the mean of the total number of cells per field was around 600. No differences were detected in the total number of cells per field among experimental groups (data not shown). The magnification used for the quantification was $20\times$, and the number of fields studied for sample was two. No differences were found in the total cell numbers among the analyzed fields per sample (data not shown).

Confocal microscopy

An LSM 510 Meta confocal laser scanner mounted on an Axio Imager Z1 microscope (Carl Zeiss) was used for confocal microscopy as previously described (55). Negative controls consisting of the tissue incubated without primary antibodies were performed for each experiment (data not shown).

Real-time quantitative PCR

Total RNA from the hypothalamus and the adrenal glands was isolated using an RNeasy mini kit (Qiagen) according to the instructions of the manufacturer. The residual genomic DNA was removed using an RNase-Free DNase set (Qiagen). Total RNA ($1 \mu\text{g}$) was reverse transcribed using the

superscript II kit according to the instructions of the manufacturer (Invitrogen). Real-time quantitative PCRs were performed using Power SYBR Green PCR master mix (Applied Biosystems) and a Chromo 4TM Real-Time system (Bio-Rad). Quantification was performed at a threshold detection line (Ct value). The Ct value for the target genes (*NOX2*) was normalized with the relative levels of *Rps9* (ribosomal protein S9) and *Tbp* (TATA-box-binding protein) mRNAs used as house-keeping genes. Triplicates were performed for each condition. Results are expressed as fold increase. The sequence of the primers used has been previously described (56).

Statistical analysis

All statistical analyses were performed using SigmaStat® 3.1 and GraphPad® 5.0 for Windows. The statistical tests are indicated in the figure legends. For all tests, a *p*-value < 0.05 was considered statistically significant. Results are expressed as means ± standard error.

As comparative results were obtained for controls at 2, 4, and 7 weeks, data of these three experimental groups have been plotted and showed as a single group (GRP) to avoid redundancy in the graphs. Statistical analysis has been performed both on single or plotted data. In both cases, the same statistical significances have been obtained.

Acknowledgments

The authors were supported by the Swiss National Foundation (Grant No. 3200A0-103725), the Italian PRIN to LT for 2009 from MIUR, the Swedish Medical Research Council, the European Union Grants MASTERSWITCH (HEALTH-F2-2008-223404), and EURATRANS (HEALTH-F4-2010-241504).

Author Disclosure Statement

The authors declare no biomedical financial interests or potential conflicts of interest relevant to the subject matter of this work. KHK is the funding member of GenKyoTex, which develops NOX inhibitors.

References

- Adams K. Pathophysiologic role of the renin-angiotensin-aldosterone and sympathetic nervous systems in heart failure. *Am J Health Syst Pharm* 61: S4–S13, 2004.
- Ahmed Z, Shaw G, Sharma VP, Yang C, McGowan E, and Dickson DW. Actin-binding proteins coronin-1a and IBA-1 are effective microglial markers for immunohistochemistry. *J Histochem Cytochem* 55: 687–700, 2007.
- Ahs F, Furmark T, Michelgard A, Langstrom B, Appel L, Wolf OT, Kirschbaum C, and Fredrikson M. Hypothalamic blood flow correlates positively with stress-induced cortisol levels in subjects with social anxiety disorder. *Psychosom Med* 68: 859–862, 2006.
- Albert NM, Yancy CW, Liang L, Zhao X, Hernandez AF, Peterson ED, Cannon CP, and Fonarow GC. Use of aldosterone antagonists in heart failure. *JAMA* 302: 1658–1665, 2009.
- Albrecht P, Lewerenz J, Dittmer S, Noack R, Maher P, and Methner A. Mechanisms of oxidative glutamate toxicity: the glutamate/cystine antiporter system xc⁻ as a neuroprotective drug target. *CNS Neurol Disord Drug Targets* 9: 973–982, 2010.
- Aldieri E, Riganti C, Polimeni M, Gazzano E, Lussiana C, Campia I, and Ghigo D. Classical inhibitors of NOX NAD(P)H oxidases are not specific. *Curr Drug Metab* 9: 686–696, 2008.
- Alexa HV. Early life stress, the development of aggression and neuroendocrine and neurobiological correlates: what can we learn from animal models? *Front Neuroendocrinol* 30: 497–518, 2009.
- Altamura AC, Boin F, and Maes M. HPA axis and cytokines dysregulation in schizophrenia: potential implications for the antipsychotic treatment. *Eur Neuropsychopharmacol* 10: 1–4, 1999.
- Asaba K, Iwasaki Y, Yoshida M, Asai M, Oiso Y, Murohara T, and Hashimoto K. Attenuation by reactive oxygen species of glucocorticoid suppression on proopiomelanocortin gene expression in pituitary corticotroph cells. *Endocrinology* 145: 39–42, 2004.
- Bedard K and Krause K. The NOX family of ROS-generating NADPH oxidases: physiology and pathophysiology. *Physiol Rev* 87: 245–313, 2007.
- Behrens M, Ali S, Dao D, Lucero J, Shekhtman G, Quick K, and Dugan L. Ketamine-induced loss of phenotype of fast-spiking interneurons is mediated by NADPH-oxidase. *Science* 318: 1645–1647, 2007.
- Behrens M, Ali S, and Dugan L. Interleukin-6 mediates the increase in NADPH-oxidase in the ketamine model of schizophrenia. *J Neurosci* 28: 13957–13966, 2008.
- Belvederi Murri M, Pariante CM, Dazzan P, Hepgul N, Papadopoulos AS, Zunszain P, Di Forti M, Murray RM, and Mondelli V. Hypothalamic-pituitary-adrenal axis and clinical symptoms in first-episode psychosis. *Psychoneuroendocrinology* 37: 629–644, 2012.
- Breen AP and Murphy JA. Reactions of oxyl radicals with DNA. *Free Radic Biol Med* 18: 1033–1077, 1995.
- Bulut M, Savas HA, Altindag A, Virit O, and Dalkilic A. Beneficial effects of N-acetylcysteine in treatment resistant schizophrenia. *World J Biol Psychiatry* 10: 626–628, 2009.
- Carlson M and Earls F. Psychological and neuroendocrinological sequelae of early social deprivation in institutionalized children in Romania. *Ann N Y Acad Sci* 807: 419–428, 1997.
- Checkley S. The neuroendocrinology of depression and chronic stress. *Br Med Bull* 52: 597–617, 1996.
- Cohen SI. Cushing's syndrome: a psychiatric study of 29 patients. *Br J Psychiatry* 136: 120–124, 1980.
- Collip D, Nicolson NA, Lardinois M, Lataster T, van Os J, and Myin-Germeys I. Daily cortisol, stress reactivity and psychotic experiences in individuals at above average genetic risk for psychosis. *Psychol Med* 41: 2305–2315, 2011.
- Connell BJ and Saleh TM. Co-administration of apocynin with lipoic acid enhances neuroprotection in a rat model of ischemia/reperfusion. *Neurosci Lett* 507: 43–46, 2012.
- Corcoran CM, Smith C, McLaughlin D, Auther A, Malaspina D, and Cornblatt B. HPA axis function and symptoms in adolescents at clinical high risk for schizophrenia. *Schizophr Res* 135: 170–174, 2012.
- Eng LF and Ghirnikar RS. GFAP and Astrogliosis. *Brain Pathol* 4: 229–237, 1994.
- Fone KCF and Porkess MV. Behavioural and neurochemical effects of post-weaning social isolation in rodents—relevance to developmental neuropsychiatric disorders. *Neurosci Biobehav Rev* 32: 1087–1102, 2008.
- Greti A. HPA axis responsiveness to stress: implications for healthy aging. *Exp Gerontol* 46: 90–95, 2011.

25. Grippio AJ and Johnson AK. Stress, depression and cardiovascular dysregulation: A review of neurobiological mechanisms and the integration of research from preclinical disease models. *Stress* 12: 1–21, 2009.
26. Gunnar M and Donzella B. Social regulation of the cortisol levels in early human development. *Psychoneuroendocrinology* 27: 199–220, 2002.
27. Herrman H, Stewart D, Diaz-Granados N, Berger E, Jackson B, and Yuen T. What is resilience? *Can J Psychiatry* 56: 258–265, 2011.
28. Hu X, Zhang D, Pang H, Caudle WM, Li Y, Gao H, Liu Y, Qian L, Wilson B, Di Monte DA, Ali SF, Zhang J, Block ML, and Hong J-S. Macrophage antigen complex-1 mediates reactive microgliosis and progressive dopaminergic neurodegeneration in the MPTP model of Parkinson's disease. *J Immunol* 181: 7194–7204, 2008.
29. Hullin R, Jerram T, Lee M, Levell M, and Tyrer S. Renin and aldosterone relationships in manic depressive psychosis. *Br J Psychiatry* 131: 575–581, 1977.
30. Hultqvist M, Sareila O, Vilhardt F, Norin U, Olsson L, Olofsson P, Hellman U, and Holmdahl R. Positioning of a polymorphic quantitative trait nucleotide in the *Ncf1* gene controlling oxidative burst response and arthritis severity in rats. *Antioxid Redox Signal* 14: 2373–2383, 2011.
31. Johnson A and Grippio A. Sadness and broken hearts: neurohumoral mechanisms and co-morbidity of ischemic heart disease and psychological depression. *J Physiol Pharmacol* 57: 5–29, 2006.
32. Kasal D and Schiffrin E. Angiotensin II, aldosterone, and anti-inflammatory lymphocytes: interplay and therapeutic opportunities. *Int J Hypertens* 2012: 829786, 2012.
33. Kehne JH and Cain CK. Therapeutic utility of non-peptidic CRF1 receptor antagonists in anxiety, depression, and stress-related disorders: evidence from animal models. *Pharmacol Ther* 128: 460–487, 2010.
34. Klomp A, Koolschijn PC, Hulshoff Pol HE, Kahn RS, and Van Haren NEM. Hypothalamus and pituitary volume in schizophrenia: a structural MRI study. *Int J Neuropsychopharmacol* 15: 281–288, 2012.
35. Krebs M, Leopold K, Hinzpeter A, and Schaefer M. Neuroprotective agents in schizophrenia and affective disorders. *Expert Opin Pharmacother* 7: 837–848, 2006.
36. Kudielka BM, Buske-Kirschbaum A, Hellhammer DH, and Kirschbaum C. HPA axis responses to laboratory psychosocial stress in healthy elderly adults, younger adults, and children: impact of age and gender. *Psychoneuroendocrinology* 29: 83–98, 2004.
37. Leng A, Feldon J, and Ferger B. Long-term social isolation and medial prefrontal cortex: dopaminergic and cholinergic neurotransmission. *Pharmacol Biochem Behav* 77: 371–379, 2004.
38. Lennart W. The relationship between the pineal gland and the pituitary-adrenal axis in health, endocrine and psychiatric conditions. *Psychoneuroendocrinology* 8: 75–80, 1983.
39. Lieberman JA, Tollefson GD, Charles C, Zipursky R, Sharma T, Kahn RS, Keefe RSE, Green AI, Gur RE, McEvoy J, Perkins D, Hamer RM, Gu H, Tohen M; HGDH Study Group. Antipsychotic drug effects on brain morphology in first-episode psychosis. *Arch Gen Psychiatry* 62: 361–370, 2005.
40. Lull M, Levesque S, Surace M, and Block M. Chronic apocynin treatment attenuates beta amyloid plaque size and microglial number in hAPP(751)(SL) mice. *PLoS One* 6: e20153, 2011.
41. Meyza KZ, Boguszewski PM, Nikolaev E, and Zagrodzka J. Age increases anxiety and reactivity of the fear/anxiety circuit in Lewis rats. *Behav Brain Res* 225: 192–200, 2011.
42. Mico J, Rojas-Corrales M, Gibert-Rahola J, Parellada M, Moreno D, Fraguas D, Graell M, Gil J, Irazusta J, Castro-Fornieles J, Soutullo C, Arango C, Otero S, Navarro A, Baeza I, Martinez-Cengotitabengoa M, and Gonzalez-Pinto A. Reduced antioxidant defense in early onset first-episode psychosis: a case-control study. *BMC Psychiatry* 11: 26, 2011.
43. Morgane PJ, Mokler DJ, and Galler JR. Effects of prenatal protein malnutrition on the hippocampal formation. *Neurosci Biobehav Rev* 26: 471–483, 2002.
44. Mullen RJ, Buck CR, and Smith AM. NeuN, a neuronal specific nuclear protein in vertebrates. *Development* 116: 201–211, 1992.
45. Myers B, McKlveen J, and Herman J. Neural regulation of the stress response: the many faces of feedback. *Cell Mol Neurobiol* 2012 DOI: 10.1007/s10571-012-9801-y.
46. Olofsson P, Holmberg J, Tordsson J, Lu S, Akerström B, and Holmdahl R. Positional identification of *Ncf1* as a gene that regulates arthritis severity in rats. *Nat Genet* 33: 25–32, 2003.
47. Olofsson P, Johansson Å, Wedekind D, Klötting I, Klinga-Levan K, Lu S, and Holmdahl R. Inconsistent susceptibility to autoimmunity in inbred LEW rats is due to genetic crossbreeding involving segregation of the arthritis-regulating gene *Ncf1*. *Genomics* 83: 765–771, 2004.
48. Owe-Larsson B, Ekdahl K, Edbom T, Ösby U, Karlsson H, Lundberg C, and Lundberg M. Increased plasma levels of thioredoxin-1 in patients with first episode psychosis and long-term schizophrenia. *Prog Neuro-Psychopharmacol Biol Psychiatry* 35: 1117–1121, 2011.
49. Queisser N and Schupp N. Aldosterone, oxidative stress, and NF- κ B activation in hypertension-related cardiovascular and renal diseases. *Free Radic Biol Med* 53: 314–327, 2012.
50. Roubos EW, Dahmen M, Kozicz Ts, and Xu L. Leptin and the hypothalamo-pituitary-adrenal stress axis. *Gen Comp Endocrinol* 177: 28–36, 2012.
51. Sapolsky R, Armanini M, Packan D, Sutton S, and Plotsky P. Glucocorticoid feedback inhibition of adrenocorticotropic hormone secretagogue release. Relationship to corticosteroid receptor occupancy in various limbic sites. *Neuroendocrinology* 51: 328–336, 1990.
52. Schen C. When mothers leave their children behind. *Harv Rev Psychiatry* 13: 233–243, 2005.
53. Schiavone S, Sorce S, Dubois-Dauphin M, Jaquet V, Colaianna M, Zotti M, Cuomo V, Trabace L, and Krause K. Involvement of NOX2 in the development of behavioral and pathologic alterations in isolated rats. *Biol Psychiatry* 66: 384–392, 2009.
54. Seckl. Prenatal glucocorticoids and long-term programming. *Eur J Endocrinol* 151: U49–U62, 2004.
55. Sorce S and Krause K-H. NOX enzymes in the central nervous system: from signaling to disease. *Antioxid Redox Signal* 11: 2481–2504, 2009.
56. Sorce S, Schiavone S, Tucci P, Colaianna M, Jaquet V, Cuomo V, Dubois-Dauphin M, Trabace L, and Krause K-H. The NADPH oxidase NOX2 controls glutamate release: a novel mechanism involved in psychosis-like ketamine responses. *J Neurosci* 30: 11317–11325, 2010.
57. Stachowiak M, Sebbane R, Stricker EM, Zigmund MJ, and Kaplan BB. Effect of chronic cold exposure on tyrosine hydroxylase mRNA in rat adrenal gland. *Brain Res* 359: 356–359, 1985.
58. Stefanska J and Pawliczak R. Apocynin: molecular aptitudes. *Mediators Inflamm* 2008: 106507, 2008.

59. Taliáz D, Loya A, Gersner R, Haramati S, Chen A, and Zangen A. Resilience to chronic stress is mediated by hippocampal brain-derived neurotrophic factor. *J Neurosci* 31: 4475–4483, 2011.
60. Tang LL YK, Yang XF, and Zheng JS. Apocynin attenuates cerebral infarction after transient focal ischaemia in rats. *J Int Med Res* 35: 517–522, 2007.
61. Tang XN, Cairns B, Cairns N, and Yenari MA. Apocynin improves outcome in experimental stroke with a narrow dose range. *Neuroscience* 154: 556–562, 2008.
62. Tarullo AR and Gunnar MR. Child maltreatment and the developing HPA axis. *Horm Behav* 50: 632–639, 2006.
63. Ueta Y, Dayanithi G, and Fujihara H. Hypothalamic vasopressin response to stress and various physiological stimuli: visualization in transgenic animal models. *Horm Behav* 59: 221–226, 2011.
64. Ulrich-Lai YM, Figueiredo HF, Ostrander MM, Choi DC, Engeland WC, and Herman JP. Chronic stress induces adrenal hyperplasia and hypertrophy in a subregion-specific manner. *Am J Physiol—Endocrinol Metab* 291: E965–E973, 2006.
65. van Winkel R, Stefanis NC, and Myin-Germeys I. Psychosocial stress and psychosis. a review of the neurobiological mechanisms and the evidence for gene-stress interaction. *Schizophr Bull* 34: 1095–1105, 2008.
66. Vilhardt F. Microglia: phagocyte and glia cell. *Int J Biochem Cell Biol* 37: 17–21, 2005.
67. Wang Q, Tompkins KD, Simonyi A, Korhuis RJ, Sun AY, and Sun GY. Apocynin protects against global cerebral ischemia-reperfusion-induced oxidative stress and injury in the gerbil hippocampus. *Brain Res* 1090: 182–189, 2006.

Address correspondence to:

Prof. Luigia Trabace
 Department of Clinical and Experimental Medicine
 University of Foggia
 Viale Luigi Pinto, 1
 c/o O.O.R.R.
 71100 Foggia
 Italy

E-mail: trabace@unifg.it

Date of first submission to ARS Central, February 13, 2012; date of final revised submission, January 13, 2013; date of acceptance, January 16, 2013.

Abbreviations Used

8OhdG = 8-hydroxy-2-deoxyguanosine
 ACTH = adrenocorticotrophic hormone
 APCN = apocynin
 CNS = central nervous system
 CRF = corticotropin-releasing factor
 GABA = γ -aminobutyric acid
 GRP = control rats (reared in group)
 HPA-axis = hypothalamic-pituitary-adrenal axis
 ISO = isolated rats
 NCF1 = neutrophil cytosolic factor 1
 NOX2 = NADPH oxidase 2
 PCR = polymerase chain reaction
 ROS = reactive oxygen species